Hamedan University of Technology
Iranian Association of Electrical and Electronics Engineers

Sustainable Energy and Artificial Intelligence

Online ISSN: 3060-8015

Journal Homepage: www.enai.hut.ac.ir

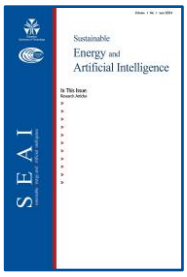

Power System Resilience Enhancement Based on Network Reconfiguration and Photovoltaic Resources Integration

Seyed Masoud Moeini, Abbas Fattahi*

Electrical and Computer Engineering Department, Hamedan University of Technology, Hamedan, Iran
** Corresponding Author: fattahi@hut.ac.ir*

Article Info

Article type:
Original Article

Article history:
Received 2026-02-05;
Revised 2026-05-29;
Accepted 2026-06-05.

How to cite this article:
Moeini, S. M. and Fattahi, A. (2026). Power System Resilience Enhancement Based on Network Reconfiguration and Photovoltaic Resources Integration. *Sustainable Energy and Artificial Intelligence*, 2(2), 131-144.
DOI: 10.61882/seai.2602-1043

Abstract

Natural disasters, such as floods and earthquakes, frequently cause widespread power outages and irreversible damage to equipment and consumers within the power industry. Ensuring a safe and uninterrupted electricity supply during such events represents a primary challenge for modern power system operators, a concept often termed network resilience. This paper proposes a network reconfiguration plan, integrated with photovoltaic (PV) resource management, to enhance the resilience of a power distribution network against natural disaster threats. The proposed approach minimizes the total expected costs, comprising both equipment repair/reinforcement and consumer outage costs, which serve as the objective function. Furthermore, the model incorporates AC power flow constraints, network reconfiguration logic, and PV resource capacity limits. Uncertainties—including active and reactive load demands, PV generation, and the availability of network components (such as main/reserve lines and PV resources)—are modeled using scenario-based stochastic programming. Scenarios are generated via the Monte Carlo method, with a subset selected using the Kantorovich reduction technique. Finally, the resulting stochastic optimization problem is formulated as a Mixed-Integer Nonlinear Programming model and solved using GAMS software. The proposed method is implemented and analyzed on 33-bus and 119-bus sample networks through four distinct case studies. Numerical results conclusively demonstrate that the integration of robust PV resources, combined with network reconfiguration, significantly improves network resilience under various natural disaster scenarios.

***Keywords*:** PV Resources; Network Reconfiguration; Network Resilience; Scenario-Based Stochastic Programming; Power System.

List of Symbols

T_{ESS} (s)	The time constant related to the ESS	T_{ESS} (s)	The time constant related to the ESS
P^{PV}, P^{DS}, P^{DL}	Active power generated by PV resources, injected from distribution substation, and flow of distribution lines	Q^{PV}, Q^{DS}, Q^{DL}	Reactive power generated by PV resources, injected from distribution substation, and flow of distribution lines
u^{PV}, u^{DS}, u^{DL}	Binary variables representing the availability of PV resources, distribution substation, and distribution lines	z	Binary variable representing the operational status of a distribution line switch (0/1, open/closed)
V, β	Magnitude and angle of bus voltage		

Constants

B	Branch-to-bus incidence matrix	B^{DL}, G^{DL}	Conductance and susceptance of distribution lines
N_{Bus}	Number of buses in the distribution network	P^{C}, Q^{C}	Active and reactive power demand
P^{NS}	Active power not supplied	$RC^{PV}, RC^{DS}, RC^{DL}$	Repair and reinforcement costs for PV resources, distribution substation, and distribution lines
$\overline{S}^{PV}, \overline{S}^{DS}, \overline{S}^{DL}$	Maximum capacity of PV resources, distribution substation, and distribution lines	$\underline{V}, \overline{V}$	Maximum and minimum voltage magnitude at buses
$VOLL$	The Value of Lost Load	ρ	Scenario occurrence probability

Indices and Sets

k, b	Bus indices	h	Hour of operation
ω	Scenario index	Bus	Set of network buses
OH	Set of operational hours	SC	Set of reduced scenarios

1. Introduction

In recent years, there have been natural disasters and cyberattacks on power systems around the world .Events such as floods and earthquakes have directly affected the physical infrastructure of power systems and have led to the collapse of systems, resulting in massive power outages and economic losses. For example, Hurricane Sandy left 7.5 million people without power across 15 states in the United States in 2012. Floods in Australia in the summer of 2010 cut electricity to approximately 150,000 people. Winter Storm Uri in February 2021 resulted in power outages for nearly 4.5 million customers in Texas and a subsequent energy crisis. Moreover, the destructive brunt of the 2022 floods in Pakistan took a heavy toll on power infrastructure, hindering electricity availability for over 10 million individuals.

Therefore, power systems need to be able to withstand the effects of rare but severe events, which is called resilience. Since the main purpose of electricity distribution companies is to deliver a clean and reliable energy supply to end users, the improvement of system resilience has recently been more focused on. This process is to reduce the load shedding, to increase the load restoration in stress, which brings the resilience as one of the most important goals in contemporary operating distribution networks.

A survey of the literature in this field shows that possible techniques for improving power system resilience can be divided into two high level categories: (i) hardening the physical infrastructure and control devices, and (ii) planning the design and operation using managerial solutions based on optimization.

The first approach model extreme events at a coarse level to find weak points of the power network, and considers high probability scenarios of component failures. Resilience indices, such as severity risk are utilized subsequently to assess system performance under perturbation [1]. Reference [2] introduces a multi-dimensional resilience index based on graph theory and the Choquet integral that captures both topological and operational aspects.

The Markov chain model is still a very popular method to approximate the state transitions of power networks during component failures in severe environments [3]. Still, emerging methods tend to incorporate machine learning and digital twin technologies for more dynamic and predictive modeling. For example, reference [4] relies on a convolutional neural network that is trained on historical weather and outage data to estimate component vulnerabilities almost in real-time.

Network resilience analysis enables the detection of system vulnerabilities in the network, leading to the identification of network segments that require the upgrading or reinforcement of system elements such as lines, transformers, etc. Reference [5] applies centrality measures from complex network theory to find critical lines and proposes targeted hardening to increase the resilience of the system. In addition, traditional hardening the use of grid-enhancing technologies is increasingly being considered. These include not only Flexible AC Transmission Systems devices [6], but also advanced power flow controllers and dynamic line rating schemes that are capable of enhancing effective network capacity under contingency conditions [7].

The recent trend in the literature towards hybrid strategies of resilience that synergistically combine infrastructure hardening with distributed resources

is today a major shift in modeling increasing resilience. The dominance of the renewable-based microgrids and distributed energy resources (DERs) are particularly highlighted for their potential in islanding critical loads and enhancing local resilience in wide-area blackout situations. Reference [8] presents case studies of how solar-plus-storage microgrids continued to power critical services during the 2023 California wildfires. In addition, reference [9] introduces a model for "resilience-as-a-service" based on mobile energy storage systems that can be dispatched to outage zones, a concept recently piloted in Florida following Hurricane Ian.

The second approach, which has recently attracted more interest, investigates the role of network reconfiguration in improving power system resilience in terms of the technical and the financial aspects. This approach aims to find the optimal planning and operation of a flexible network structure for resilience enhancement using maneuver and sectionalizing switches, considering operating conditions and generation unit availability. Generation resource availability is paramount at all levels of system recovery including stabilization of the electrical parameters, reconnection of transmission and distribution network elements, and supplying critical loads during natural disasters [10,11]. Hence, network reconfiguration is very important in increasing the adequacy and availability of connected generation sources when subjected to severe condition. In this sense, microgrids in distribution systems and coordinated generation resources management have been considered as promising techniques for improving the flexibility of operation and network resilience. The ability of microgrids to separate from the main grid and operate in island mode has recently received much attention as a feasible and efficient solution for reducing the effects of regionwide blackouts induced by natural disasters [12, 13]. Thus, increasing of flexibility in power generation control using DERs and energy storage systems (ESSs) in microgrids will greatly aid network recovery processes after extreme events [14, 15].

A next generation approach involves the co-scheduling of DERs, ESSs, and network reconfiguration to enhance the post-event load restoration and recovery time under an uncertain operating condition. Reference [14] presented a new reconfiguration strategy at the energy storage system level, coordinating ESSs with renewable energy sources (RESs) to improve distribution system resilience. The integrated framework of this work is designed to establish a flexible system responding to the high-impact low-probability (HILP) event, and formulated as a stochastic nonlinear non-convex optimization model with probabilistic constraints. Likewise, Reference [16] introduced distribution network stochastic planning for distributed generation integration and the network reconfiguration considering resilience enhancement. Their approach features two-stage optimization: the location and size of distributed generators and resilient infrastructure are identified in the first stage, and the best network reconfiguration is introduced in the second stage to reduce load shedding in disaster situation.

To increase resilience for floods and earthquakes, synchronous distributed generation, robust distribution lines, and network reconfiguration have been integrated into a planning framework based on AC optimal power in reference [17]. The objective function considers the total investment cost, the operational cost, and the expected energy not supplied (EENS) due to the flood and earthquake conditions. The uncertainties in respect of load demand, energy prices and component availability are handled utilizing scenario-based stochastic programming. The optimization problem is first linearized and then divided into two main subproblems. The first subproblem focuses on network reconfiguration, while the second addresses operating costs and load curtailment. In a related effort, reference [18] generalized this approach by employing a hybrid stochastic–robust optimization to better handle uncertainty. Furthermore, reference [19] studied the effect of co-optimizing distribution system planning with energy storage system and found that ESS can significantly enhance the resilience of distribution system.

Recently, reference [20] presented a two-stage stochastic mixed-integer linear programming (MILP) model that integrates resilience-oriented planning for active distribution systems. This probabilistic model develops upon traditional resilience planning framework by directly incorporating into consideration regional extreme weather risks when designing and operating distribution networks. One interesting feature of this work is that a significant amount of system generation resilience during natural disasters is provided by distributed generators used as backup generation resources. But this requires up-front investment in infrastructure that is not fully used until a rare event of large magnitude occurs. Hence the continuing research on less costly ways to boost resilience, primarily through flexible reconfiguration, better use of energy storage, and more advanced operational coordination.

Unlike traditional fossil-fueled backup generators, which are inflexible, have high operation and maintenance costs, and emit greenhouse gases, PV-based microgrids can provide fast, local, and clean backup power to critical loads in extreme events [21, 22]. This feature is especially vital in disaster-prone regions, because a slow recovery of power can endanger public safety, emergency services, and the local economy. Although substantial progress has been made in microgrid control and resilience design, there are still a number of critical deficiencies that have yet to be filled in the literature. Some existing works studied a few isolated aspects such as stochastic load management, PV output uncertainty, or islanded microgrid operation, but did not address these issues in an integrated network reconfiguration paradigm under extreme events [23, 24]. Besides, the total cost to the economy due to repair and loss of services caused by network outages is not accounted for traditionally and traditional methods do not usually consider ac power flow constraints, PV operational limits and multi-stage stochastic uncertainties in an integrated optimization model. All methods are either based on an oversimplified system model using DC approximations or deterministic methods, which makes them not applicable to real distribution networks with relatively high PV penetration.

An additional important gap in the literature is the contribution of PV generation to active resilience improvement in comparison with traditional fossil-fueled backup units. Although the fossil generators have long been the standard answer to emergency backup needs, they have their own limitations such as availability of fuel, startup times, and environmental implications. On the other hand, when suitable network reconfiguration strategies are adopted, PV arrays can offer a continuous backup power source with minimal carbon emissions and geographical flexibility, which leads to a reduction in outage times and in the negative economic impacts caused by repairing. Furthermore, PV integration allows for adaptive islanding and selective load pick-up, which may further enhance system survivability in the event of cascading failures or component failures.

To tackle these issues, a new optimal planning model for distribution system resilience improvement through network reconfiguration and PV-based microgrids is presented in this paper. The framework considered minimizes network outage costs and repair costs of damaged components, subject to ac power flow constraints, line and transformer limits, PV operational features, and reconfiguration constraints. To deal with uncertainties of load demand, PV power, and equipment availability under natural disasters, e.g., floods and earthquakes, a scenario-based stochastic programming model is applied. Scenarios are generated using Monte Carlo simulation and reduced by the Kantorovich method to keep the computational burden manageable. The nonlinear model is linearized and formulated as MILP problem and solved by GAMS efficiently. By explicitly prioritizing PV integration over fossil-fueled backup units and incorporating it in a stochastic, network-reconfiguration framework, this paper bridges a major research gap and offers a systematic, computationally tractable, and practical tool for distribution system planners and operators. The method contributes not only to improving the networks resilience to HILP events, but also to the greening of the networks through sustainable utilization of RESs considering technical and social goals.

The rest of the paper is organized as: After the introduction, in Section 2 the planning formulation is described, with the objective functions and the constraints applicable to the network, PV resources, reconfiguration, and resilience. Furthermore, the linearized versions of the resulting optimization problem are given. In Section 3, the application of the proposed approach to two example networks in different cases is demonstrated. Subsequently, numerical investigations follow and the results are interpreted and discussed. Finally, Section 4 concludes the paper and gives suggestions for future work.

2. Proposed Methods

In this section, an optimization model is proposed to enhance the resilience of power distribution systems against floods and earthquakes, aiming to minimize load shedding resulting from such natural disasters. The proposed model integrates network reconfiguration with optimal scheduling of power generation from PV resources and supply from distribution substations. Considering that floods and earthquakes can cause damage to distribution lines, PV units, and substations, the model also accounts for the availability cost associated with these components. Accordingly, the operational status of line maneuver switches, as well as the active and reactive power injections into the

network, are optimized to achieve the minimum possible power outage during extreme events. Hence, the proposed approach provides a resilience enhancement framework formulated as an optimal operation planning model under natural disaster conditions. The detailed formulation of the optimization problem, including the objective function and associated constraints, is presented in the following subsections.

2-1. Objective Function

The objective function of the proposed planning model is provided in Equation (1):

$$\min \sum_{\omega \epsilon SC} \rho_{\omega} \left(\sum_{b \epsilon Bus} \left(\begin{array}{l} RC_{b}^{PV} u_{b,\omega}^{PV} + \\ RC_{b}^{DS} u_{b,\omega}^{DS} + \\ \sum_{k \epsilon Bus} RC_{b,k}^{DL} u_{b,k,\omega}^{DL} + \\ VOLL \times \sum_{h \epsilon OH} P_{b,h,\omega}^{NS} \end{array} \right) \right) \quad (1)$$

As shown in Equation (1), the objective function of the problem consists of four distinct components. The first three components relate to the repair, maintenance, and reinforcement costs for the PV resources, distribution substation, and distribution lines, respectively. The last component of the objective function models the cost of load shedding, commonly referred to as EENS. Additionally, the binary parameter *u* in Equation (1) represents the operational status of the equipment, which is used as an indicator of equipment availability under natural disaster conditions. A value of *u*=1 signifies that the equipment is operational and connected to the network, while *u*=0 indicates that the equipment is damaged and disconnected from the network [17].

2-2. Network Operation Constraints

The network operation constraints, including AC power flow equations and network safety requirements, are presented in Equation (2) to (10):

$$\begin{aligned} & P_{b,h,\omega}^{DS} u_{b,\omega}^{DS} + P_{b,h,\omega}^{PV} u_{b,\omega}^{PV} \\ & \quad - \sum_{k \epsilon Bus} B_{b,k} P_{b,k,h,\omega}^{DL} u_{b,k,\omega}^{DL} \\ & \quad = P_{b,h,\omega}^{C} - P_{b,h,\omega}^{NS} \end{aligned} \quad (2)$$

$$\forall\, b, h, \omega$$

$$\begin{aligned} & Q_{b,h,\omega}^{DS} u_{b,\omega}^{DS} + Q_{b,h,\omega}^{PV} u_{b,\omega}^{PV} \\ & \quad - \sum_{k \epsilon Bus} B_{b,k} Q_{b,k,h,\omega}^{DL} u_{b,k,\omega}^{DL} \\ & \quad = Q_{b,h,\omega}^{C} \end{aligned} \quad (3)$$

$$\forall\, b, h, \omega$$

$$\begin{aligned} & P_{b,k,h,\omega}^{DL} \\ & = \left\{ G_{b,k}^{DL} \left(V_{b,h,\omega}\right)^2 \right. \\ & - V_{b,h,\omega} V_{k,h,\omega} \{ G_{b,k}^{DL} \cos\left(\beta_{b,h,\omega} - \beta_{k,h,\omega}\right) \\ & \left. + B_{b,k}^{DL} \sin\left(\beta_{b,h,\omega} - \beta_{k,h,\omega}\right) \} \right\} \end{aligned} \quad (4)$$

$$\forall\, b, h, \omega$$

$$\begin{aligned} & Q_{b,k,h,\omega}^{DL} \\ & = \left\{ -B_{b,k}^{DL} \left(V_{b,h,\omega}\right)^2 \right. \\ & + V_{b,h,\omega} V_{k,h,\omega} \{ B_{b,k}^{DL} \cos\left(\beta_{b,h,\omega} - \beta_{k,h,\omega}\right) \\ & \left. + G_{b,k}^{DL} \sin\left(\beta_{b,h,\omega} - \beta_{k,h,\omega}\right) \} \right\} \end{aligned} \quad (5)$$

$$\forall\, b, h, \omega$$

$$\beta_{b,h,\omega} = 0 \qquad \forall\, b = \text{SlackBus}, h, \omega \quad (6)$$

$$\sqrt{\left(P_{b,k,h,\omega}^{DL}\right)^2 + \left(Q_{b,k,h,\omega}^{DL}\right)^2} \leq \overline{S}_{b,k}^{DL} u_{b,k,\omega}^{DL} \quad (7)$$

$$\forall\, b, k, h, \omega$$

$$\sqrt{\left(P_{b,k,h,\omega}^{DS}\right)^2 + \left(Q_{b,k,h,\omega}^{DS}\right)^2} \leq \overline{S}_{b}^{DS} u_{b,\omega}^{DS} \quad (8)$$

$$\forall\, b = \text{Slack Bus}, h, \omega$$

$$\underline{V} \leq V_{b,h,\omega} \leq \overline{V} \qquad \forall\, b, h, \omega \quad (9)$$

$$0 \leq P_{b,h,\omega}^{NS} \leq P_{b,h,\omega}^{C} \qquad \forall\, b, h, \omega \quad (10)$$

Constraints (2) to (6) represent the AC power flow equations in the distribution network. Specifically, Equations (2) and (3) define the active and reactive power balance at the network buses, Eqs .(4) and (5) describe the active and reactive power flow through the lines, and Equation (6) determines the voltage angle at the slack bus. Moreover, the operational safety constraints of network, including the apparent power limits of lines and the distribution substation, the voltage magnitude limits of buses, and the resilience bounds of the network, are incorporated into the planning through Constraints (7) to (10). It is noteworthy that, assuming the distribution network is connected to the upstream network via the distribution substation located at the slack bus and variables P^{DS} and Q^{DS} are set to zero for all other buses [17, 25].

2-3. Network Reconfiguration Constraints

The switching operations for maneuver switches, which are essential for enhancing network resilience, must comply with the constraints shown in Equations (11) and (12):

$$\sum_{b,k \epsilon Bus} z_{b,k,h,\omega} \leq N_{Bus} - 1 \qquad \forall\, b, k, h, \omega \quad (11)$$

$$z_{b,k,h,\omega} \leq u_{b,k,\omega}^{DL} \qquad \forall\, b, k, h, \omega \quad (12)$$

Equation (11) ensures the radial structure of the network during reconfiguration. In this equation, the binary variable *z* represents the status of the distribution line switch (1 for closed, 0 for open). A value of 1 (0) for *z* indicates that the line is connected (disconnected) from the network.

Equation (12) indicates that z can only take a value of 1 if u^{DL}=1, meaning that the corresponding line is available for reconfiguration [17].

2-4. PV Resource Constraints

The primary constraint on power generation from PV resources is related to the capacity of the DC/AC converter between the PV panels and the network, as shown in Equation (13):

$$\sqrt{\left(P^{PV}_{b,h,\omega}\right)^2 + \left(Q^{PV}_{b,h,\omega}\right)^2} \leq \bar{S}^{PV}_{b,k}\, u^{PV}_{b,\omega} \quad \forall\, b, h, \omega \tag{13}$$

According to Equation (13), it is assumed that PV sources allow to operate in maximum power point tracking mode while simultaneously participating in reactive power management [26].

2-5. Uncertainty Modeling

To effectively address the stochastic nature of uncertain variables inherent in the proposed planning framework, a scenario generation-based uncertainty modeling approach is utilized. The key uncertain parameters considered in this study encompass:

1) Load Consumption: Active and reactive power consumption.
2) Renewable Generation: Active power output from PV resources.
3) Component Availability: The operational status (availability) of distribution lines, distribution substation, and PV resources.

Initially, a large set of scenarios is generated using Monte Carlo simulations. Within each scenario, the specific values for load and PV generation are drawn based on their respective mean and standard deviation. Specifically, the probability distribution for load consumption is modeled using a Normal distribution function, whereas the probability distribution for PV power generation is modeled via a Beta distribution function [17]. Furthermore, the uncertain operational status of physical equipment is determined using the Forced Outage Rate (FOR) for each component under natural disaster conditions, which is modeled by a Bernoulli probability distribution function [19].

Subsequent to scenario generation, a scenario reduction method based on the Kantorovich technique is applied. This method is implemented in three main sections. First, the pairwise Euclidean distances between all generated scenarios are calculated. Then, for each scenario, the nearest neighboring scenario and the corresponding Euclidean distance are identified. Subsequently, based on the Kantorovich distance criterion, defined as the product of the Euclidean distance a given scenario and its occurrence probability, the scenario with the minimum Kantorovich distance is eliminated. The occurrence probability of the removed scenario is then transferred to its nearest neighboring scenario. This process is iteratively repeated on the reduced scenario set obtained after each iteration. To terminate the scenario reduction process, the cumulative Kantorovich error, calculated as the summation of the Kantorovich distances of the eliminated scenarios, is compared with a predefined threshold value denoted by ε_{max} [27]. This step selectively retains a representative, reduced set of scenarios that are closely spaced in the sample space, which are then used as the input for the proposed planning.

3. Case Studies and Results

To evaluate the proposed planning methodology, two standard test power systems the 33-bus and 119-bus networks were selected for analysis. The resilience of each network was assessed under four distinct scenarios, designed to isolate the impact of key mitigation strategies:

Study I: Resilience assessment conducted without considering PV sources and network reconfiguration.

Study II: Resilience assessment with PV sources integrated, but without network reconfiguration.

Study III: Resilience assessment without PV sources, but with network reconfiguration.

Study IV: Resilience assessment incorporating both PV sources and network reconfiguration.

3-1. Problem Data

Fig. 1 illustrates the standard 33-bus and 119-bus radial distribution networks, including the locations of the installed PV resources. In the 33-bus (119-bus) test system, the base power is set to 1 MVA (10 MVA) and the base voltage is 6.6 kV (11 kV). The permissible voltage range for these networks is set within the interval [0.95,1.05] per unit. Furthermore, the capacities of the installed PV resources are 0.5 MVA (0.8 MVA) in the 33-bus (119-bus) test network, respectively.

The specifications for the lines and distribution substation of these test networks, along with the active and reactive peak load data for each bus, are provided in reference [18]. The hourly load and PV generation values would be obtained by multiplying the respective peak values by their corresponding daily rates [17, 28]. The expected daily profile for the system load and PV generation rate is plotted in Fig. 2

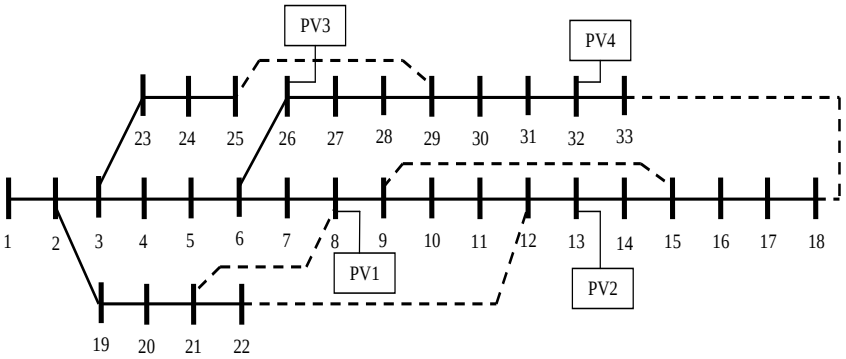

(a)

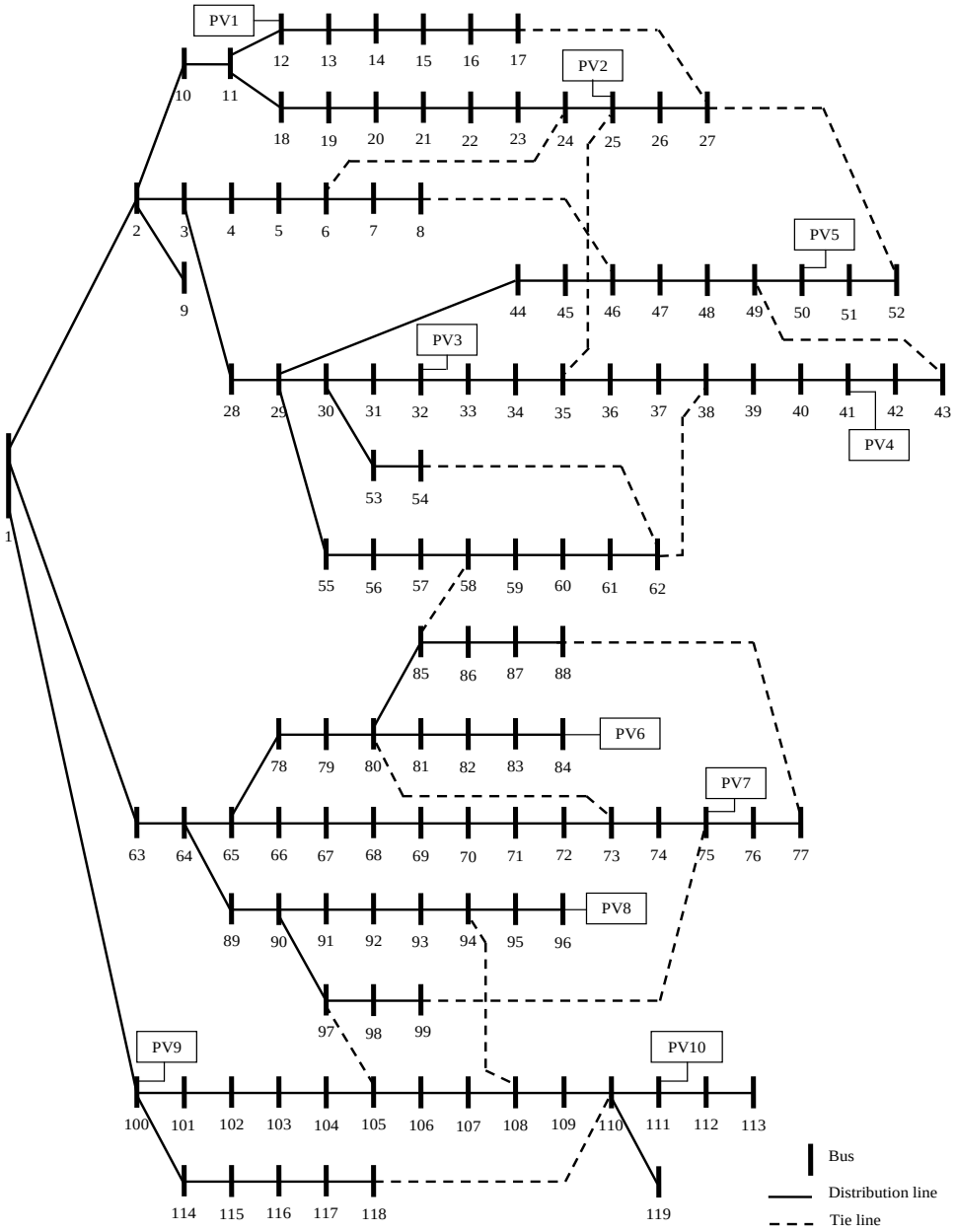

(b)

Fig. 1. Sample networks for case studies, a) 33-bus network, and b) 119-bus network

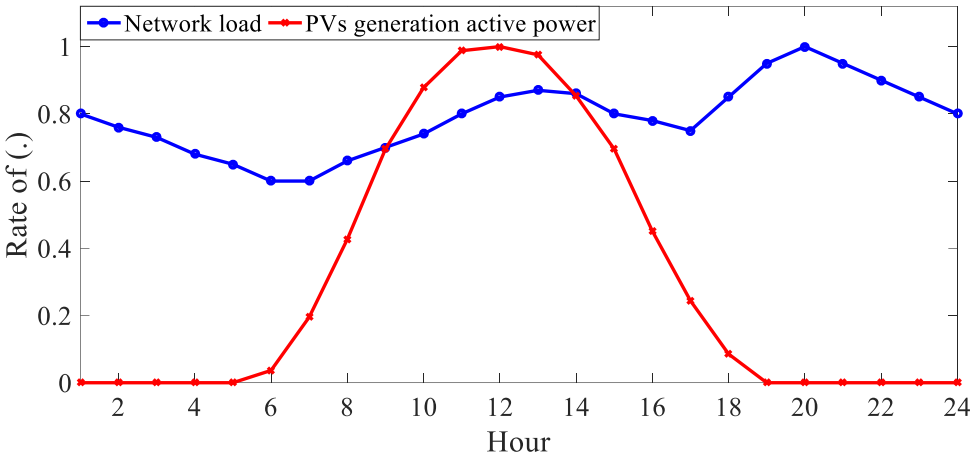

Fig. 2. Daily system load and PV generation rates for the sample networks

Since natural disasters affect only specific segments of the network, the following exposure scenarios are assumed for the test systems. In the 33-bus network, buses 11–16 and 23–24 (19-21 and 29-32) are assumed to be exposed to earthquakes (floods). In the 119-bus network, earthquakes (floods) may occur at buses 21–27 and 28–33 (39–43 and 70–73). The repair and reinforcement costs for primary lines, backup lines, and PV sources located in flood-prone and earthquake-prone areas are set at 80$/MVA, 50$/MVA, and 100$/MVA, respectively [18]. Assuming the distribution substation is not located in a disaster-prone area, and its repair cost is set to zero. The FOR values for primary lines, backup lines, and PV sources in these areas is assumed to be 5%, 5%, and 3%, respectively. A standard deviation of 10% is adopted for the uncertainties associated with both load and PV generation. To achieve high resilience, the penalty factor for VOLL is set to 1000 $/MWh.

3-2. Numerical Results

To perform the case studies using the proposed stochastic planning approach, 1000 scenarios were initially generated for the uncertainties in load, PV generation, and equipment availability via Monte Carlo simulation. Subsequently, using the Kantorovich method and setting the value of ε_{max} to 0.05, 40 representative scenarios were selected and applied to the case studies. Furthermore, the optimization problem for the proposed planning was solved for each case study using the GAMS software with the BONMIN module.

3-2-1. Resilience Assessment

Table 1 reports the results of the proposed planning model for both the 33-bus and 119-bus networks across the four defined case studies presented in Section 3.

The results presented in Table 1 indicate that equipment repair costs in both sample networks are the lowest in Case Study I and reach their maximum values in Case Study IV. This is primarily because, in Case Study I, only distribution lines are exposed to potential damage from floods and earthquakes. In contrast, in the other case studies, both PV generation resources and reserve distribution lines (relevant to network reconfiguration) are also subject to damage from natural disasters. Furthermore, consumer outage costs exhibit the opposite trend: they are highest in Case Study I and lowest in Case Study IV. This outcome is attributed to the significant load loss experienced by consumers connected to downstream buses when line failures occur due to floods and earthquakes in Case Study I. Conversely, in Case Study IV, the presence of robust, locally deployed PV resources throughout the network, coupled with the ability to effectively reroute power through resilient reserve lines via network reconfiguration, prevents load shedding in critical areas during fault conditions. For instance, in the 33-bus network, consumer outage costs in Case Study IV are reduced by 96.5% compared to Case Study I; for the 119-bus network, this reduction is approximately 98%.

When comparing Case Studies II and III, the results suggest that the most substantial reduction in load loss and outage costs is achieved when only PV resources are integrated into the network (Case Study II). Conversely, equipment repair and reinforcement costs remain lower when only reserve lines are utilized for network reconfiguration (Case Study III).

Table 1. Expected costs of equipment repair and consumer outages in the 33-bus and 119-bus networks for the defined case studies

Distribution Network	Case Study	Equipment Repair Cost ($)	Consumer Outage Cost ($)	Total Cost ($)
33-bus	I	491.6	11,984	12,475.6
	II	621.6	846.3	1,467.9
	III	506.8	2,021.4	2,528.2
	IV	636.8	499.9	1,136.7
119-bus	I	1,475.1	34,053.3	35,528.4
	II	1,655.5	1,188.0	2,843.5
	III	1,509.4	3,012.3	4,521.7
	IV	1,689.8	682.0	2,371.8

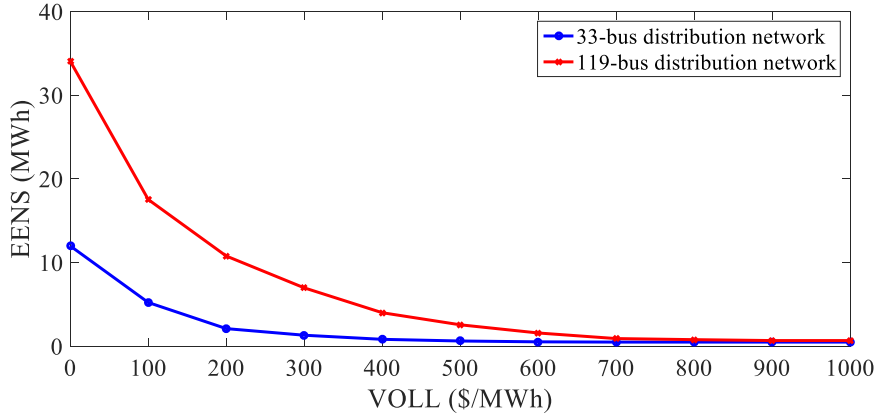

Fig. 3. EENS curve as a function of the VOLL for the 33-bus and 119-bus sample networks evaluated under the conditions of Case Study IV

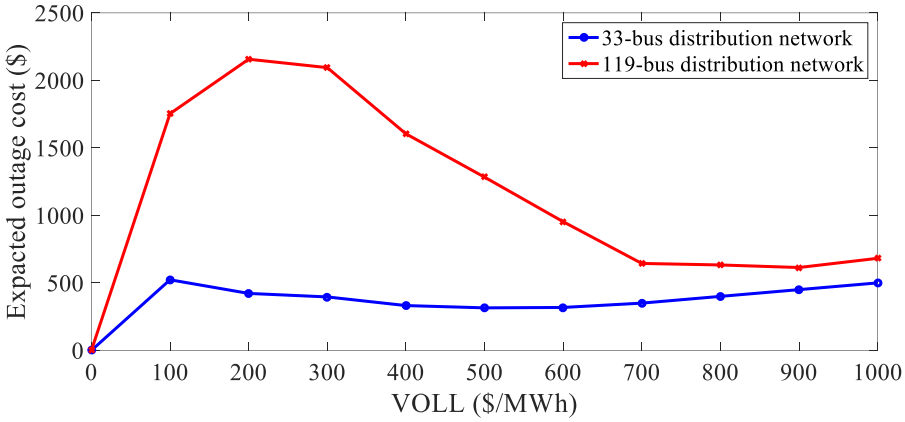

Fig. 4. Consumer outage cost curve as a function of the VOLL for the 33-bus and 119-bus sample networks under the proposed approach in Case Study IV

Overall, the findings in Table 1 demonstrate that the expected resilience cost (defined as the sum of expected repair and outage costs) achieved through the proposed stochastic planning approach (Case Study IV) is reduced by approximately 90% and 93% in the 33-bus and 119-bus networks, respectively, when benchmarked against Case Study I. This reduction signifies a substantial improvement in network resilience within an economically optimal framework.

3-2-2. Sensitivity Analysis

Fig. 3 illustrates the EENS curve as a function of the VOLL for both the 33-bus and 119-bus sample networks under the conditions of Study IV.

Analysis of the results, as depicted in Fig. 3, reveals an inverse relationship between the VOLL penalty and EENS: as the VOLL price increases, the resulting EENS diminishes. Notably, beyond a threshold of 700 $/MWh for VOLL, the quantity of lost load, or EENS, exhibits negligible change, suggesting system behavior reaches an asymptote. Separately, Fig. 4 presents the consumer outage cost curve plotted as a function of VOLL.

As shown in Fig. 4, in the 33-bus network, the consumer outage cost initially increases as VOLL rises to 100$/MWh. Conversely, in the 119-bus

network, this initial increase persists up to 200$/MWh. Within these initial ranges, the influence of the increasing VOLL penalty on the total cost is less significant than the effect of the EENS. For VOLL values between 100$/MWh and 600$/MWh (for the 33-bus network) and between 200$/MWh and 900$/MWh (for the 119-bus network), the relationship reverses. Within these ranges, the impact of the rising VOLL on consumer outage costs outweighs the EENS. Outside of these two defined ranges, the EENS contribution remains constant. Consequently, in the latter part of the range where EENS is constant, increasing VOLL directly leads to a monotonic increase in the calculated outage costs. Based on this trend analysis, the optimal VOLL value that minimizes the consumer outage cost is determined to be 600 $/MWh forthe33-busnetworkand 900 $/MWh for the 119-bus network.

Fig. 5 subsequently presents the expected network resilience cost curve as a function of VOLL.

As illustrated in Fig. 5, the trend of the expected network resilience cost curve with respect to VOLL closely mirrors the pattern observed in the consumer outage cost analysis presented in Fig. 4. A comparative inspection of the two figures reveals that the resilience cost curve consistently lies a fixed vertical distance above the consumer outage cost curve for all VOLL values. This uniform upward shift quantitatively confirms that the equipment repair cost component is independent of the VOLL valuation.

3-2-3. Performance Analysis of PV Resources and Network Reconfiguration

The daily profiles of active and reactive power generation from the PV resources in the 33-bus and 119-bus sample networks under the proposed resilience-oriented planning approach are illustrated in Fig. 6.

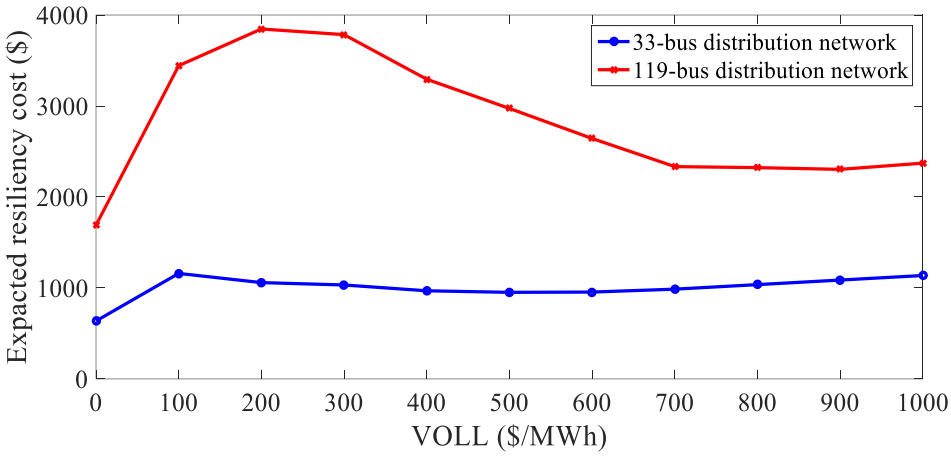

Fig. 5. Network resilience cost curve as a function of the VOLL for the 33-bus and 119-bus sample networks evaluated in Case Study IV

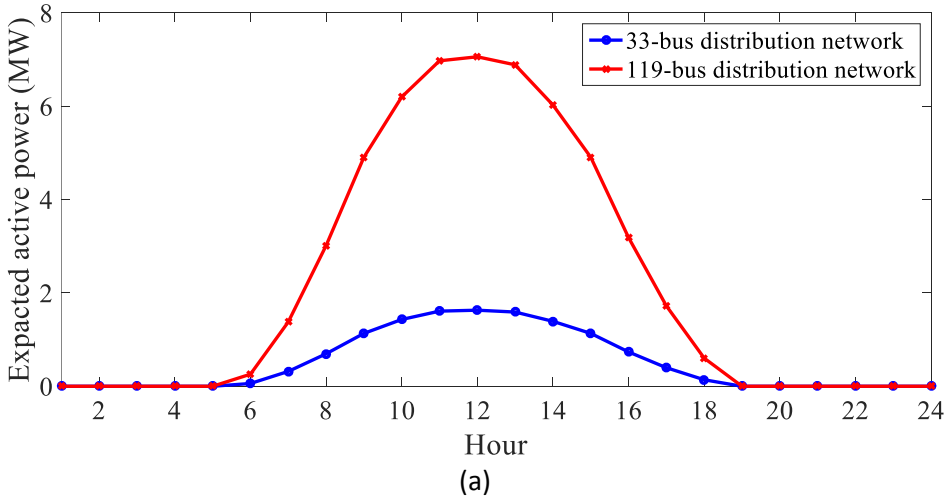

(a)

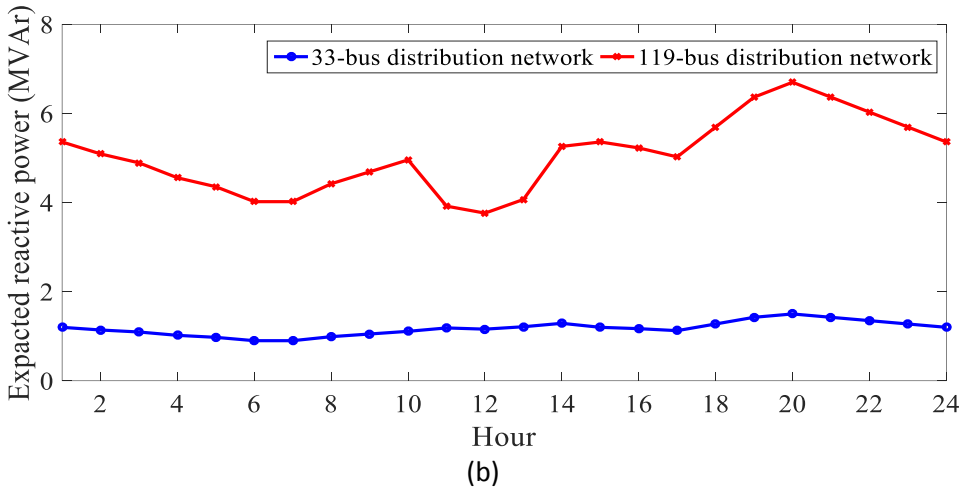

Fig. 6. Daily expected power generation curves of the PV resources: (a) active power and (b) reactive power for the 33-bus and 119-bus sample networks in Case Study IV

As illustrated in Fig. 6(a), the expected hourly pattern of active power generation from the PV resources follows the production rate profile presented in Fig. 2. Nevertheless, the maximum total active power generated by these resources is lower than their installed capacity in both test systems — 2 MVA for the 33-bus network and 8 MVA for the 119-bus network. This reduction results from the disconnection of certain PV units located in flood- and earthquake-prone areas during specific disaster scenarios.

In Fig. 6(b**)**, the reactive power generation profile of the PV resources exhibits a pattern similar to the daily load-factor curve shown in Fig. 2. This similarity suggests that, depending on their available capacity, the PV resources can effectively contribute to compensating a portion of the network's reactive power demand throughout the day.

Furthermore, Table 2 presents the status of network reconfiguration during disaster conditions, expressed through the operational performance of reserve distribution lines for both the 33-bus and 119-bus test systems.

As detailed in Table 2, all reserve lines in the 33-bus network have transitioned from the 'off' to the 'on' state. Conversely, in the 119-bus network, only 6 of the 13 total reserve lines switched from 'off' to 'on'.

3-2-4. Network Operational Indices

Table 3 presents a comparative overview of key operational indices specifically energy losses, maximum voltage drop, maximum overvoltage, and the EENS resilience index for both the 33-bus and 119-bus sample networks across the defined case studies.

Table 2. Reserve line performance status for 33-bus and 119-bus Sample Networks under Case Study IV

Sample Network	Tie Line Between Buses	Performance Status in All Operating Hours
33-bus Network	9 and 15	On
	8 and 21	On
	12 and 22	On
	25 and 29	On
119-bus Network	18 and 33	On
	6 and 24	On
	17 and 27	Off
	27 and 52	On
	8 and 46	On
	25 and 35	Off
	43 and 49	On
	58 and 65	Off
	38 and 62	On
	54 and 62	Off
	77 and 88	Off
	73 and 80	On
	94 and 108	Off
	75 and 99	Off
	110 and 118	Off

Table 3. Expected operational Indices for the 33-bus and 119-bus Sample Networks

Sample Network	Case Study	Energy Losses (MWh)	Max Voltage Drop (p.u.)	Max Overvoltage (p.u.)	EENS (MWh)
33-bus Network	I	4.432	0.087	0.000	11.9840
	II	3.436	0.054	0.013	0.8463
	III	4.034	0.084	0.000	2.0214
	IV	3.082	0.052	0.012	0.4999
119-bus Network	I	122.760	0.092	0.000	34.0533
	II	89.870	0.061	0.016	1.1880
	III	114.460	0.088	0.000	3.0123
	IV	81.940	0.059	0.015	0.6820

As shown in Table 3, the proposed planning approach (Case Study IV) yields substantial improvements over Case Study I. Specifically, it reduces energy losses by approximately 30.5% in the 33-bus sample network and 33.2% in the 119-bus sample network, while simultaneously decreasing the maximum voltage drop by 40.2% and 38.9%, respectively. These positive impacts on energy loss and voltage regulation are directly attributed to the integration of PV resources, a trend also observable in Case Study II. Furthermore, the maximum overvoltage in Case Study IV is 0.012 p.u. (33-bus) and 0.015 p.u. (119-bus), again reflecting the benefit of PV integration. Most notably, the EENS is drastically reduced by approximately 96.5% (33-bus) and 98% (119-bus) compared to Case Study I, confirming the significant role of PV resources in enhancing overall network resilience and operational indices.

4. Conclusions

This study delivers a novel contribution by resolving the identified research gap concerning the co-optimization of resilience enhancement and infrastructure investment within distribution networks characterized by high penetration of PV resources. Main contribution of this paper lies in formulating and solving an AC-constrained, scenario-based stochastic programming model that explicitly leverages PV integration for disaster resilience, thereby obviating the dependency on conventional, fossil fuel-dependent synchronous backups. The optimization formulation, solved efficiently for the 33-bus and 119-bus test systems via GAMS, successfully minimizes expected consumer outage costs subject to probabilistic component availability. The quantitative results unequivocally demonstrate the efficacy of this approach: catastrophic outage costs are diminished by 96.5% and 98.0%, respectively, across the two benchmark networks. Crucially, this enhanced resilience is achieved with a justifiable fiscal allocation, incurring only a 29.5% (33-bus) and 14.5% (119-bus) increase in anticipated repair and reinforcement expenditures. In summary, this work validates that a holistic, integrated planning approach, prioritizing PV-supported microgrid functionality, not only yields substantial improvements in standard operational metrics (voltage profiles, losses) but also establishes a quantifiable, economically sound blueprint for future-proofing electrical infrastructure against extreme climate events.

References

[1] Wang, Y., Li, X., Smith, J., & Liu, Z. (2023). A comprehensive review of power system resilience: Indices, frameworks, and enhancement strategies. *IEEE Access, 11*, 25488–25510.

[2] Chen, L., & Rahimi, M. (2023). A graph-based multi-criteria resilience assessment framework for power grids under compound hazards. *International Journal of Electrical Power & Energy Systems, 145*, 108502.

[3] Zhang, H., Zhao, J., Kumar, S., & Nguyen, T. (2023). Markovian modeling of grid component failures under sequential hurricane and flooding events. *IEEE Transactions on Power Systems, 38*(2), 1123–1134.

[4] Patel, R., Gupta, A., & Singh, M. (2023). Deep learning for predictive resilience: Real-time vulnerability assessment using CNNs and satellite data. *Applied Energy, 334*, 120678.

[5] Kumar, S., & Bose, A. (2023). Identifying critical transmission lines using electrical centrality and cascading failure analysis. *Electric Power Systems Research, 214*, 108891.

[6] Li, J., Wang, K., & Zhao, L. (2023). Coordinated control of FACTS devices for transient stability enhancement in resilience-oriented grids. *IEEE Transactions on Smart Grid, 14*(1), 223–235.

[7] Nguyen, F., & Smith, T. (2023). Dynamic line rating and topology optimization for congestion relief during extreme weather. *Renewable and Sustainable Energy Reviews, 171*, 113024.

[8] National Renewable Energy Laboratory. (2024). *Community resilience through renewable microgrids: Lessons from recent wildfire and hurricane responses* (NREL/TP-5C00-88012).

National Renewable Energy Laboratory.
[9] Johnson, M., Roberts, L., & Carter, E. (2023). Mobile energy storage for rapid outage response: A resilience-as-a-service framework. *Joule, 7*(4), 789–805.
[10] Panteli, M., & Mancarella, P. (2020). The grid: Stronger, bigger, smarter? Presenting a conceptual framework of power system resilience. *IEEE Power and Energy Magazine, 18*(3), 58–66.
[11] Dehghanian, P., Wang, Z., Wang, J., & Zhang, Y. (2021). A survey on power system resilience: Definitions, concepts, and applications. *IEEE Transactions on Smart Grid, 12*(4), 3455–3468.
[12] Lei, S., Wang, J., Chen, C., & Hou, Y. (2020). Mobile emergency generator pre-positioning and real-time allocation for resilient distribution systems. *IEEE Transactions on Smart Grid, 11*(6), 5071–5083.
[13] Zhang, Y., Xu, Y., Dong, Z. Y., & Wong, K. P. (2020). Robust microgrid planning for resilient distribution systems. *IEEE Transactions on Smart Grid, 11*(1), 362–372.
[14] Nazemi, M., Dehghanian, P., Lu, X., & Chen, C. (2021). Uncertainty-aware deployment of mobile energy storage systems for distribution grid resilience. *IEEE Transactions on Smart Grid, 12*(4), 3200–3214.
[15] Gholami, A., Aminifar, F., & Shahidehpour, M. (2023). Enhancing resilience of distribution systems using coordinated distributed energy resources, energy storage, and network reconfiguration. *Electric Power Systems Research, 216*, 109057.
[16] Ghasemi, M., Kazemi, A., Gilani, M. A., & Shafie-khah, M. (2021). A stochastic planning model for improving resilience of distribution systems considering master–slave distributed generators and network reconfiguration. *IEEE Access, 9*, 78859–78872.
[17] Shahbazi, A., Aghaei, J., Pirouzi, S., & Shafie-khah, M. (2021). Effects of resilience-oriented design on distribution networks operation planning. *Electric Power Systems Research, 191*, 106902.
[18] Shahbazi, A., Aghaei, J., & Shafie-khah, M. (2021). Hybrid stochastic–robust optimization model for resilient architecture of distribution networks against extreme weather conditions. *International Journal of Electrical Power & Energy Systems, 126*, 106576.
[19] Shahbazi, A., Aghaei, J., Pirouzi, S., & Shafie-khah, M. (2021). Holistic approach to resilient electrical energy distribution network planning. *International Journal of Electrical Power & Energy Systems, 132*, 107212.
[20] Ghosh, P., & De, M. (2024). Resilience-oriented planning for active distribution systems: A probabilistic approach considering regional weather profiles. *International Journal of Electrical Power & Energy Systems, 158*, 109976.
[21] Hamidieh, M., & Ghassemi, M. (2022). Microgrids and resilience: A review. *IEEE Access, 10*, 106059–106080.
[22] Domínguez-García, J. L., Pepiciello, A., Paradell, P., & Ivanova, A. (2023). Dynamic microgrids for strengthening power system resilience. *IEEE Smart Grid Magazine*, 1–7.
[23] Younesi, A., Shayeghi, H., Safari, A., & Siano, P. (2020). Assessing the resilience of multi-microgrid based widespread power systems against natural disasters using Monte Carlo simulation. *Energy, 207*, 118220.
[24] Kizito, R., Liu, Z., Li, X., & Sun, K. (2022). Multi-stage stochastic optimization of islanded utility microgrids design after natural disasters. *Operations Research Perspectives, 9*, 100235.
[25] Hamidpour, H., Pirouzi, S., Safaee, S., Norouzi, M., & Lehtonen, M. (2021). Multi-objective resilient-constrained generation and transmission expansion planning against natural disasters. *International Journal of Electrical Power & Energy Systems, 132*, 107193.
[26] Polat, S., Bıyık, E., & Öztura, H. Ş. (2025). Optimal active and reactive power scheduling for inverter-integrated PV and BESS under inverter current constraints. *Electric Power Systems Research, 245*, 111629.
[27] Tavakoli, A., & Karimi, A. (2023). Development of Monte-Carlo-based stochastic scenarios to improve uncertainty modelling for optimal energy management of a renewable energy hub. *IET Renewable Power Generation, 17*(5), 1139–1164.
[28] Ouédraogo, A., Zouma, B., Ouédraogo, E., Guissou, L., & Bathiébo, D. J. (2021). Individual efficiencies of a polycrystalline silicon PV cell versus temperature. *Results in Optics, 4*, 100101.

Biography

Seyed Masoud Moeini received the M.Sc. degree in Electrical Engineering from Hamedan University of Technology, Hamedan, Iran, in 2022. He is a Professional Electrical Engineer holding a Grade-1 Engineering License. His research interests include power systems, distribution system resilience, distributed energy resources, and smart grids.

Abbas Fattahi received the M.Sc. and Ph.D. degrees in electrical engineering from Sharif University of Technology, Tehran, Iran, in 1999 and 2008, respectively. Since 2009, he has been a faculty member with Hamedan University of Technology, Hamedan, Iran. His current research interests include power system planning and energy resources.